文献4

XMRV is present in malignant prostatic epithelium and is associated with prostate cancer, especially high-grade tumors

Robert Schlaberg[a,1], Daniel J. Choe[b], Kristy R. Brown[a], Harshwardhan M. Thaker[b], and Ila R. Singh[a,b,2]

[a]Department of Pathology and Cell Biology, Columbia University Medical Center, 622 West 168th Street, New York, NY 10032; and [b]Department of Pathology, University of Utah, Emma Eccles Jones Medical Research Building, 15 North Medical Drive East, Salt Lake City, UT 84112

Communicated by Stephen P. Goff, Columbia University College of Physicians and Surgeons, New York, NY, July 20, 2009 (received for review April 29, 2009)

Xenotropic murine leukemia virus–related virus (XMRV) was recently discovered in human prostate cancers and is the first gammaretrovirus known to infect humans. While gammaretroviruses have well-characterized oncogenic effects in animals, they have not been shown to cause human cancers. We provide experimental evidence that XMRV is indeed a gammaretrovirus with protein composition and particle ultrastructure highly similar to Moloney murine leukemia virus (MoMLV), another gammaretrovirus. We analyzed 334 consecutive prostate resection specimens, using a quantitative PCR assay and immunohistochemistry (IHC) with an anti-XMRV specific antiserum. We found XMRV DNA in 6% and XMRV protein expression in 23% of prostate cancers. XMRV proteins were expressed primarily in malignant epithelial cells, suggesting that retroviral infection may be directly linked to tumorigenesis. XMRV infection was associated with prostate cancer, especially higher-grade cancers. We found XMRV infection to be independent of a common polymorphism in the *RNASEL* gene, unlike results previously reported. This finding increases the population at risk for XMRV infection from only those homozygous for the *RNASEL* variant to all individuals. Our observations provide evidence for an association of XMRV with malignant cells and with more aggressive tumors.

Gleason | immunohistochemistry | retrovirus | RNaseL | xenotropic

Prostate cancer is the most common form of nonskin cancer in U.S. men (1). The lifetime risk for developing prostate cancer is ~1 in 6 (2) in the United States, and globally, 3% of men die of prostate cancer (3). Morbidity and mortality from prostate cancer are likely to grow further, given increasing longevity. Epidemiologic studies indicate that infection and inflammation may play a role in the development of prostate cancer (4, 5). A search for viral nucleic acids in prostate cancers led to the identification of xenotropic murine leukemia virus–related virus (XMRV) in ~10% of samples tested (6). Because only malignant tissues were analyzed in the initial report, an association of XMRV with prostate cancer could not be addressed. Our analysis of 233 cases of prostate cancers and 101 benign controls showed an association of XMRV infection with prostate cancer, especially with more aggressive tumors. XMRV proteins were almost exclusively expressed in malignant epithelial cells. Only rarely did we find XMRV proteins in benign stromal cells, in contrast to a previous report (6).

XMRV was originally discovered in patients with a reduced activity variant of the *RNASEL* gene, and a strong correlation between this variant (R462Q) and the presence of XMRV was reported: 89% of XMRV-positive cases and only 16% of XMRV-negative cases were homozygous (QQ) for this variant in a total of 86 cases (6). Our study of 334 cases allowed us to establish the independence of XMRV infection and the R462Q variant. This finding moves the population at risk for XMRV infection from a small, genetically predisposed fraction homozygous for the R462Q *RNASEL* variant to all men. Sequence comparisons have classified XMRV as a gammaretrovirus with a high similarity to murine leukemia viruses. We present experimental evidence that XMRV is indeed a gammaretrovirus. Gammaretroviruses cause leukemias and sarcomas in multiple rodent, feline, and primate species but have not yet been shown to cause cancers in humans. Taken together, our findings provide evidence consistent with a direct oncogenic effect of this recently discovered retrovirus. If established, a direct role for XMRV in prostate cancer tumorigenesis would open up opportunities to develop new diagnostic markers as well as new methods to prevent and treat this cancer with antiretroviral therapies or vaccines.

Results

A Molecular Clone of XMRV Infects Human Prostate Cells. We constructed pXMRV1, a full-length XMRV molecular clone, using 2 overlapping clones from patient isolate VP62 (6) [gift of Don Ganem, University of California, San Francisco (UCSF)]. pXMRV1 was transfected into 293T cells. Reverse transcriptase (RT) activity was detected in the supernatant within 1–2 days of transfection (Fig. 1*A*), indicating the release of viral particles. These were inoculated onto naive 293T cells and LNCaP cells, a human prostate cancer cell line (American Type Culture Collection CRL-1740). Viral release from infected LNCaP cells was first seen on day 7 postinoculation and peaked at day 12. No particles were released from similarly inoculated 293T cells up to day 14. pXMRV1 is therefore an infectious molecular clone, and XMRV replicates efficiently in human prostate cells.

XMRV Particles Have Type-C Retrovirus Morphology. Particles released from XMRV-infected cells closely resembled those of a gammaretrovirus, Moloney murine leukemia virus (MoMLV), in size and morphology (Fig. 1 *B–E*). XMRV particles had an average diameter of 137 nm (SD = 9 nm), a spherical to somewhat pleomorphic shape, and characteristic lipid envelopes. The majority of particles contained an electron-dense, polygonal core with an irregular outline (average diameter 83 nm, SD = 8 nm), resembling mature type-C retroviral cores (Fig. 1*C*). Cores defined as "immature," i.e., spherical with an electron-lucent center, were also seen (Fig. 1*D*). A "railroad track," a term used to describe immature MoMLV cores (7), and formed by the radial alignment of the N- and C-terminal halves of the CA protein, was also seen in immature XMRV cores (Fig. 1*D*, arrowhead). These striking ultrastructural similarities between XMRV and MoMLV (Fig. 1*E*) suggest that the 2 viruses are assembled in a very similar manner.

XMRV Proteins, Except for Env, Closely Resemble Those of MoMLV. We identified XMRV proteins and defined their molecular weights by comparing Western blots of lysed XMRV and MoMLV virions probed with antisera specific to XMRV or to MoMLV Gag proteins (Fig. 1 *F* and *G*). In accordance with their high (~90%) sequence similarities, the molecular weights of XMRV and MoMLV Gag proteins were found to be very similar. We identified a 75-kDa band as the surface unit (SU) of the envelope (Env) protein, using rabbit antiserum specific to XMRV-Env SU. This antiserum did not react with the MoMLV-SU, consistent with the lower sequence similarity (54%) of the corresponding Env proteins and the general tendency of Env proteins to show greater evolutionary divergence, as compared to Gag or Pol proteins.

Author contributions: H.M.T. and I.R.S. designed research; R.S., D.J.C., and K.R.B. performed research; R.S., H.M.T., and I.R.S. analyzed data; and R.S. and I.R.S. wrote the paper.

The authors declare no conflict of interest.

Freely available online through the PNAS open access option.

[1]Present address: Department of Pathology, University of Utah, Salt Lake City, UT 84112.

[2]To whom correspondence should be addressed. E-mail: ila.singh@path.utah.edu.

This article contains supporting information online at www.pnas.org/cgi/content/full/0906922106/DCSupplemental.

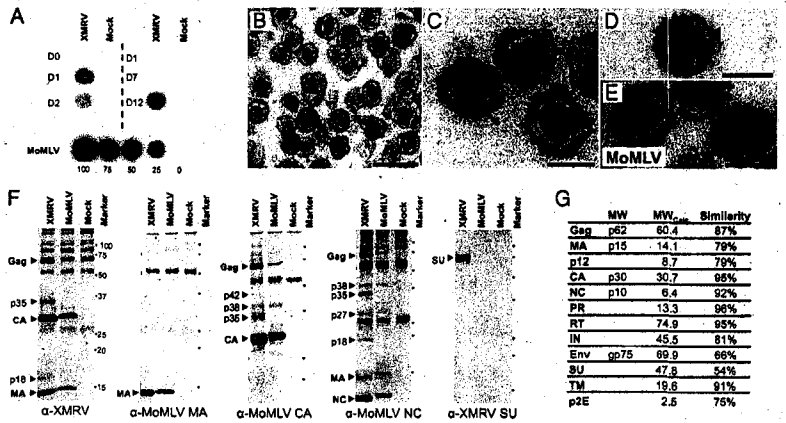

Fig. 1. The XMRV molecular clone produces infectious particles with morphology and composition similar to MoMLV. (*A*) Viral release from cells transfected or inoculated with pXMRV1 or XMRV, respectively. (*Left*) Reverse transcriptase (RT) activity in culture supernatants from cells transfected with pXMRV1 or control EGFP plasmid. (*Right*) RT activity from LNCaP cells inoculated with XMRV. (*Lower*) RT activity from NIH 3T3 cells chronically infected with MoMLV shown for comparison. (*B–E*) Transmission electron microscopy of XMRV particles (*B*), mature XMRV cores (*C*), immature XMRV core, with "railroad track" marked by arrowhead (*D*), and MoMLV particles with mature ("M") and immature ("I") cores (*E*). (*F*) Western blot analysis of lysed XMRV and MoMLV virions, using antisera to XMRV whole virus, MoMLV-CA, MoMLV-MA, MoMLV-NC, and XMRV-Env SU. Comparison of blots allows identification of intermediates of Gag proteolysis, e.g., p27 (MA-p12), p42 (p12-CA), and p38 (CA-NC). (*G*) Molecular weights of XMRV proteins as calculated by Western blot analysis and by sequence prediction and similarity between XMRV and MoMLV proteins. [Scale bars: 250 nm (*B*) and 100 nm (*C–E*).]

XMRV Proviral DNA Is Detected in 6% of Human Prostate Cancers; Viral Loads of XMRV Are Low. Our quantitative (q)PCR was designed to efficiently amplify XMRV proviral DNA from formalin-fixed, paraffin-embedded (FFPE) tissues. Primers and probes were chosen in a region of the integrase gene that is 100% conserved between all 3 published XMRV isolates and yet shares at most 80% similarity with the most closely related murine retroviral sequences (Fig. S1*A*). A common forward primer was used with 2 different reverse primers to allow for sequence differences in clinical isolates. Our qPCR was specific for XMRV sequences and did not amplify murine or human endogenous retroviruses; no amplification products were seen when using C57BL/6 mouse genomic DNA or human placental DNA as template. We tested the sensitivity of our qPCR assay in 2 ways. First, in the presence of excess human placental DNA, we could consistently detect 50 copies of the XMRV proviral clone and 5 copies 50% of the time (Fig. S1*B*). Second, because formalin fixation and embedding in paraffin compromise DNA quality, we also used fixed templates to test sensitivity. When DNA from FFPE human prostate tissue sections was spiked with known dilutions of DNA from fixed and embedded XMRV-infected, cultured cells, we consistently detected 1–2 infected cells per qPCR sample (Fig. S1*C*). We developed a second qPCR targeting the single-copy gene–vesicle-associated membrane protein 2 (VAMP2) to test for DNA integrity and amplification inhibitors [details in supporting information (*SI*) *Text*].

To estimate the prevalence of XMRV in men with and without prostate cancer, we analyzed 233 consecutively accessioned prostate cancers and 101 cases of transurethral resection of the prostate (TURP) as benign controls (Fig. S1*D*). We detected XMRV DNA in 14 (6.2%) cases of prostate cancer and in 2 (2.0%) controls. We determined XMRV proviral loads in these tissues. Using XMRV plasmid DNA as a standard, we estimated that qPCR-positive prostate cancers contained 1–10 copies of XMRV DNA per 660 diploid cells (see *Materials and Methods* and Fig. S1*E*). Because the number of tumor cells in any given section varies widely between tumors and even between different areas in the same tumor, it is impossible to estimate how many copies of XMRV DNA are present in each *tumor* cell. Using FFPE XMRV-infected cells as standards, we calculated that each 10-μm section from a prostate cancer contained the same amount of proviral DNA as 6–7 XMRV-infected cultured cells.

XMRV Protein Is Expressed in 23% of Prostate Cancers and Is Predominantly Seen in Malignant Epithelium. We developed XMRV-specific antisera and used them for immunohistochemistry (IHC). We first used XMRV-infected and uninfected cells that were mixed at different ratios and fixed in formalin and embedded in paraffin to mimic prostate tissue sections. We saw granular cytoplasmic staining in cells in proportion to the percentage of infected cells in the corresponding mixtures (Fig. 2 *A–C*). No staining was seen in uninfected cells or with preimmune serum (Fig. S2 *A* and *B*), confirming the specificity of our assay. We next performed IHC on prostate samples from XMRV qPCR-positive cases. We saw the same cytoplasmic granular pattern in tissues as in infected cultured cells (Fig. 2 *D* and *E*). Antiserum from a second rabbit resulted in identical staining. No staining was seen with preimmune serum (Fig. 2*F*).

We tested tissue sections from all 334 cases of prostate cancer and

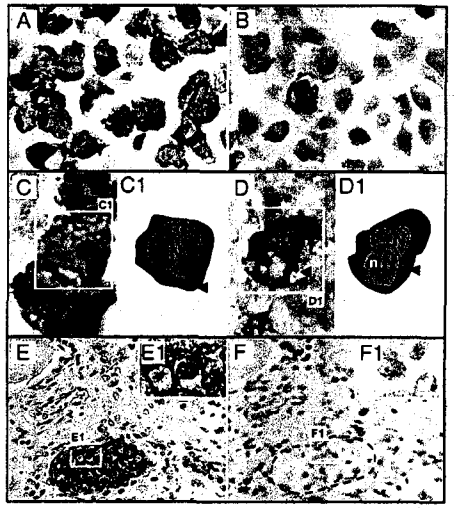

Fig. 2. XMRV proteins detected in infected cultured cells and in prostate cancer tissue by IHC, using anti-XMRV antiserum. Counterstaining with hematoxylin reveals blue nuclei. (A and B) XMRV-infected cells: 100% infected (A) and 1% infected (B). (C) Cultured infected cells at higher magnification show cytoplasmic granular staining, represented diagrammatically in C1 (arrowhead, granules). (D–F) Human prostate cancers with clusters of malignant epithelial cells (E), with Inset at higher magnification (E1). Granular staining pattern seen at higher magnification. (F and F1) Adjacent section stained with preimmune serum from the same rabbit. N, nucleus; n, nucleolus.

controls with benign prostatic hyperplasia. We found XMRV protein expression in 54 (23%) cases with prostate cancer and in 4 (4%) controls (Fig. 4*A*). In contrast to a previous report (6) that found XMRV-specific staining only in nonmalignant stromal cells, we observed XMRV-specific staining predominantly in malignant prostatic epithelial cells. XMRV proteins were expressed in epithelial cells in 46 tumors (85%), in both epithelial and stromal cells in 4 tumors (7.5%), and exclusively in stromal cells in another 4 tumors (7.5%). Of the 4 controls, XMRV expression was seen in epithelial cells in 3 and in both epithelial and stromal cells in 1 case. Epithelial cells expressing XMRV protein usually belonged to a single acinus or to a few adjacent acini. The proportion of cells expressing XMRV protein in a given tissue section varied widely (Fig. 3 *A–G*) but positive cells always represented a minority of cells on the slide. The vast majority of IHC-positive epithelial cells showed the same granular staining pattern of the entire cytoplasm that was seen in cultured cells (Fig. 3 *A–F*). However, the staining intensity and the subcellular pattern varied between cases, ranging from intense staining of the entire cytoplasm (Fig. 3*E*) to more discrete granular staining (Fig. 3 *C* and *D*), with some unusual staining patterns (Fig. 3*G*). In summary, XMRV proteins were expressed in 23% of prostate cancers and 4% of controls. Protein expression was seen in clusters of malignant epithelial cells and very rarely in stromal cells (Fig. 3 *H* and *I*).

Presence of XMRV Correlates with Prostate Cancer and Higher Tumor Grade. We tested for a correlation of XMRV positivity (by qPCR or IHC) with the presence, grade, and stage of prostate cancer. XMRV positivity was 5-fold higher in cancer than in benign controls (odds ratio = 5.7, $P < 0.0001$, Fig. 4*A*). We also tested for a correlation between XMRV positivity and tumor grade as measured by the Gleason score. We saw a correlation between XMRV positivity and higher-grade cancers (Fig. 4*B*). Of the 233 cases with cancer, we found XMRV positivity in 18% of Gleason 6 tumors, 27% of Gleason 7 tumors, 29% of Gleason 8 tumors, and 44% of Gleason 9 tumors (χ^2-test for trend, $\chi^2 = 3.466$, $P = 0.06$, df = 1). Because only 1 case was a Gleason 10, it was not included in the analysis.

Most radical prostatectomy specimens contain relatively low pathological tumor–node–metastasis (TNM) stage cancers, because surgical treatment is not usually performed for higher stages. This is reflected in the distribution of tumor stages (pT) in our series: 75% pT2, 23% pT3, and 2% pT4. XMRV was detected in 25% of stage pT2 tumors and in 32% of pT3 tumors. Of the 5 cases with a pT4 stage, 1 (20%) was XMRV positive (Fig. 4*C*). This moderately increased prevalence of XMRV in advanced stage cancers was not statistically significant. Our sample had very few cases with nodal (N) metastasis and no cases with known distant metastases (M), preventing an investigation of a possible association of XMRV with higher N and M stages. We saw no association between XMRV infection and age at diagnosis (Fig. 4*D*).

XMRV Infection Is Independent of the R462Q Polymorphism of *RNASEL*. XMRV was initially discovered in prostate cancers from men homozygous for a common variant of the antiviral enzyme RNase L. This R462Q amino acid substitution results in a 3-fold reduction of enzymatic activity (8). In their study of 86 men with prostate cancer, Urisman et al. reported that 89% of XMRV-positive cases were homozygous for the R462Q variant (QQ) as compared to 16% of XMRV-negative cases (6). We profiled our 334 cases for the RNase L R462Q variant. The distribution was similar between cases with prostate cancer and controls (42.9% RR, 47.2% RQ, and 9.9% QQ in cancers vs. 52.5% RR, 40.6% RQ, and 6.9% QQ in controls, Fig. 4*E*). There was also no difference in allelic distribution between XMRV PCR-positive (50% RR, 43% RQ, and 7% QQ) and PCR-negative cases (42.7% RR, 47.4% RQ, and 10% QQ; Fig. 4*E*). The 2 XMRV-positive controls had RR alleles. When IHC was used to define XMRV-positive and -negative cases, the relative allelic distributions were also similar. We thus found no association between the presence of XMRV and the RNase L R462Q variant.

Discussion

XMRV is a candidate infectious agent for causing prostate cancer. On the basis of sequence comparison, XMRV was classified as a xenotropic murine gammaretrovirus. We present the first experimental evidence in support of this classification. The morphology of XMRV particles was very similar to MoMLV, a related murine gammaretrovirus. Protein products of the 2 viruses had similar molecular weights, and antisera to most proteins of each virus. The notable exception to this was the SU portion of Env, which determines host specificity and sets xenotropic viruses apart from other related murine viruses. XMRV SU-specific antisera did not cross-react with MoMLV-SU, and the 2 proteins share only a 54% similarity (as opposed to 75–96% similarity for other viral proteins). Our findings thus support the classification of XMRV as a xenotropic murine gammaretrovirus.

We developed 2 sensitive and specific assays for the detection of XMRV in tissues. We used these qPCR and IHC assays to demonstrate the presence of XMRV DNA or proteins in 27% of cases in the largest series of human prostate cancers analyzed thus far. We show that XMRV proteins are expressed almost exclusively in cancerous epithelial cells. Moreover, the presence of XMRV correlated with more aggressive, i.e., higher-grade tumors. These findings provide support for a possible oncogenic effect of XMRV and are crucial for designing studies to investigate mechanisms of transformation.

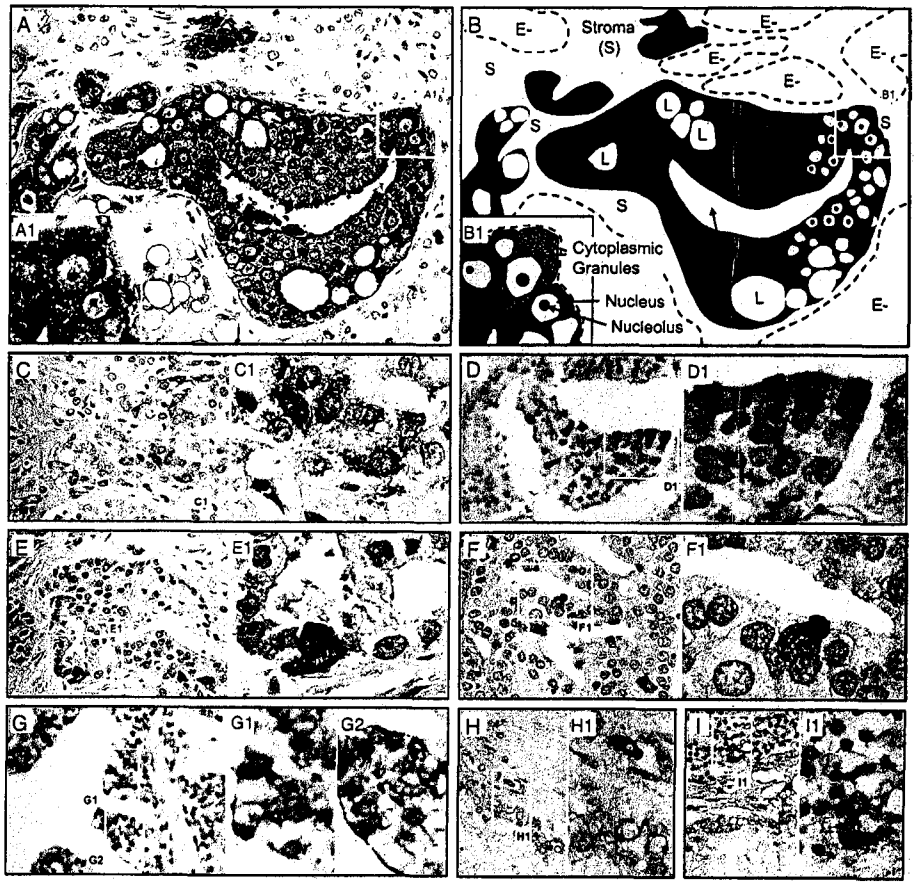

Fig. 3. XMRV proteins are expressed primarily in malignant epithelial cells and very rarely in stromal cells. (A and B) IHC of a section from a qPCR-positive prostate cancer (A) and its diagrammatic representation (B). Nuclei of malignant cells are large and contain ≥1 large nucleoli (B). Multiple acini of malignant epithelial cells (E+) stain positive. All cells within these acini show intense staining. The stroma (S) and a few other acini (E−) are unstained. Insets (A1 and B1) show corresponding fields at higher magnification, with granular cytoplasmic staining pattern in several malignant epithelial cells. (C) A different field from the same sample as in A shows the range of XMRV protein expression in various acini: fewer cells expressing less protein but the same granular staining pattern. (D–F) Three additional representative samples with different frequencies of malignant epithelial cell clusters and different extents of XMRV protein expression. The intracellular staining pattern remains granular in all. (G) Staining limited to part of the cytoplasm of malignant epithelial cells in a subset of samples, as in this sample from which the XMRV clone VP62 was isolated, courtesy of R. H. Silverman and C. Magi-Galluzzi, Cleveland Clinic (6). (H and I) Scattered rare stromal cells showing cytoplasmic staining were seen close to malignant cells (H) or within inflammatory infiltrates (I).

The fraction of cases positive for XMRV by qPCR (6%) was lower than by IHC (23%). This variation can be attributed to sampling differences in conjunction with very low viral loads. For the qPCR, detection rates depend on the *proportion* of XMRV-infected cells in the tissue. DNA from infected cells gets diluted in DNA from uninfected cells, thus limiting sensitivity if only a few cells in the sample harbor XMRV. However, qPCR allows a rapid survey of large numbers of tissue samples. In contrast, IHC detects individual XMRV-infected cells, avoiding the dilution effect of PCR. However, the number of cells analyzed is much smaller by IHC (a 5-μm section vs. a 100-μm section for DNA extraction) and only actively replicating virus can be detected. Because XMRV produces focal, low-level infections, the 2 assays complement each other and using both is likely to lead to the most accurate estimate of prevalence.

Two of our findings differ significantly from the initial report on XMRV (6). First, we found XMRV proteins in malignant epithelial cells in contrast to initial reports of XMRV proteins in nonmalig-

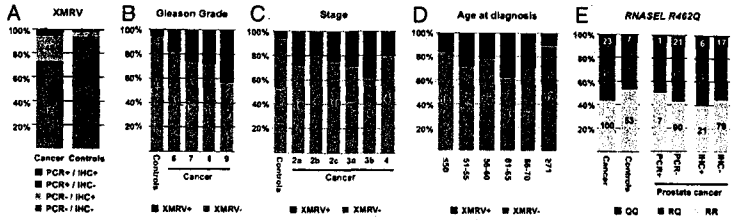

Fig. 4. XMRV DNA and proteins were more prevalent in prostate cancer than in controls, and especially frequent in high-grade cancers, and there was no correlation between presence of XMRV and any particular *RNASEL* genotype. (*A*) Number of prostate cancers or controls that were positive or negative for XMRV, either by qPCR or by IHC. (*B–D*) XMRV-positive cases (by either IHC or qPCR) correlated with Gleason grades (*B*), tumor stage (*C*), or age at diagnosis (*D*). (*E*) Presence of XMRV DNA or protein and the *RNASEL* genotype. Relative frequencies of RR, RQ, and QQ alleles in *RNASEL* at residue 462 were compared in prostate cancer cases and controls (*Left*), in cancers that tested positive or negative for XMRV DNA by qPCR (Center), and in cancers that tested positive or negative for XMRV proteins by IHC (*Right*). Cases are shown as percentages of total on the *y* axis and as number of cases within columns.

nant stromal cells. This can be mostly explained by our use of XMRV-specific antiserum instead of the monoclonal antibody to spleen focus-forming virus Gag protein used in the initial report. We were also able to detect XMRV in malignant epithelium from a case in the initial report (Fig. 3*G*), supporting the notion that antisera specific to XMRV offer a more sensitive means of viral detection. Second, we did not see any association of XMRV with the RNase L R462Q polymorphism as described initially. Methodological differences might account for this discrepancy. We tested prostate cancers for the presence of XMRV DNA and protein, whereas Urisman et al. used a nested RT-PCR to amplify viral RNA. It is conceivable that the reduced-activity variant of RNase L has a more significant effect on the levels of XMRV RNA, rather than on infection per se. Given low viral loads, the chance of detecting XMRV RNA may, therefore, be greater in homozygous individuals. Alternatively, the strength of association may depend on allelic frequencies and prevalence of XMRV. The distribution of RNase L R462Q alleles differed significantly between the 2 studies (23% QQ, 16% RQ, 61% RR in the study by Urisman et al. vs. 10% QQ, 43% RR, and 47% RQ in this study). Consistent with our findings, a survey in Northern European patients identified 2 individuals with XMRV; neither was homozygous for R462Q (9). The independence of XMRV infection from the RNase L R462Q variant indicates that all individuals may be at risk for XMRV infection, not just the ~10% of the population that is homozygous for R462Q. Preventive and antiviral measures will thus benefit a much larger at risk population.

Our finding that XMRV is present in cancerous epithelial cells has important implications for pathogenesis. If XMRV plays a role in prostate cancer development, but infects only nonmalignant stromal cells in the tumor as previously reported, new mechanisms of retroviral oncogenesis would need to be invoked. This finding has discouraged investigation of a causal role of XMRV in prostate cancer thus far. While such a new mechanism is possible, our findings are immediately compatible with classical mechanisms of cell transformation by retroviruses. Retroviruses follow 3 distinct pathways when transforming cells. The first is transduction by an oncogene, where a cell-derived oncogene such as *src* in the viral genome causes rapid transformation. The second is via an essential retrovirus gene transactivating cellular growth-promoting genes, as in the case of the Tax protein of HTLV-I that induces T cell leukemia (10, 11), or the Env protein of Jaagsiekte sheep retrovirus that induces lung cancer in sheep (12). XMRV contains no recognizable oncogene, but we do not understand each XMRV protein enough to rule out any role it might play in transactivation. Finally, there is the insertional activation of a cellular oncogene, a mechanism followed by most leukemia-causing murine gammaretroviruses. Multiple rounds of viral infection are typically needed for the activating insertion to occur. Cells containing the activating insertion are selected over others, leading over time to a distinctly clonal population. While a small number of XMRV integration sites have been sequenced from human prostate cancers (13, 14), no evidence of clonality has emerged yet. Furthermore, the mechanism of insertional activation requires that each cancer cell contains a provirus or, at a minimum, the regulatory sequences from 1 LTR. We estimated that qPCR-positive prostate cancers contained 1–10 copies of XMRV DNA per 660 diploid cells. Because the number of malignant cells in any section varies widely between cases and even between different sections in the same prostate, it is impossible to estimate how many copies of XMRV DNA are present in each *cancer* cell. Our IHC data show that not all malignant cells express XMRV proteins, a finding with 2 possible explanations. It is possible that the malignant cells that lack XMRV protein expression were never infected by XMRV at all—a possibility that is incompatible with any known mechanism of insertional activation by murine gammaretroviruses. Alternatively, it is possible that some XMRV-infected cells lose large portions of their proviral DNA over time, as seen in tumors induced by avian leukosis virus (ALV). In these ALV-induced tumors, an absence of proviral sequences essential for production of viral RNA in most cells, coupled with the absence of viral RNA in tumors, indicates that expression of viral genes is not required for maintenance of the tumor phenotype (15). More studies are required to determine whether XMRV plays any causal role in prostate cancer or whether the presence of the virus in malignant prostatic epithelium is simply a function of its preferential replication in prostate cancer cells.

In line with a slow mechanism for oncogenesis, detection of XMRV in 6% of our controls might indicate that XMRV causes cancer only after a long induction period. Alternatively, these cases may have cancer in an unsampled area of the prostate: TURP removes periurethral tissue whereas cancer usually arises in the periphery of the prostate. It is also possible that XMRV infection does not always lead to cancer. Because our study protocol involves de-identified samples, follow-up of these XMRV-positive controls is not possible.

The finding that XMRV replicates efficiently in a cell line derived from human prostate cancer but not in other human cell lines suggests a viral tropism that warrants further investigation. Is the virus associated with cancers in tissues other than the prostate or in gynecologic malignancies? How is XMRV transmitted? These are all intriguing questions that deserve further exploration. There is growing evidence that current prostate cancer screening algorithms result in early detection of cancers but do not effectively reduce mortality (16, 17). Many cases of prostate cancer are unlikely to manifest themselves during the patient's lifetime. There is a clear need for better markers to detect cancers that pose a significant health threat and to specifically target these for therapy. XMRV, because of its association with more aggressive cancers, might provide such a marker. Furthermore, there are often cases where a screening test is positive, but no tumor is detected on multiple biopsies, leaving the patient and his physician with no clear guidelines. A second XMRV-specific marker might provide further guidance. Large epidemiologic studies are needed to investigate correlation of XMRV with prostate cancer prognosis. The recognition that human papilloma viruses most often initiate cervical carcinomas has focused efforts on viral detection for early diagnosis and on preventive vaccination. Similarly, a determination that a retrovirus can cause prostate cancer would focus efforts on preventing transmission, antiviral therapy, and vaccine development. The pharmacological inhibition of viral replication, as achieved with HIV-1, could dramatically limit the pathological consequences of chronic viral infection.

Materials and Methods

Creating an Infectious Clone of XMRV. Overlapping partial clones AM-2–9 and AO-H4 derived from patient isolate VP62 (6) (gift of Don Ganem, UCSF) were used to generate pXMRV1, a full-length clone of XMRV with a CMV promoter (details of construction and sequencing are in *SI Text*).

Cell and Virus Production and Assay for Reverse Transcriptase Activity. 293T cells were maintained in DMEM and LNCaP cells in RPMI, both supplemented with 10% FBS, L-glutamine (2.2 mM), penicillin (100 units/mL), and streptomycin (100 μg/mL). Cells were transfected with plasmid pXMRV1 or control plasmid pEGFP-C1 (Clontech), using Lipofectamine PLUS (Invitrogen) following manufacturer's directions. Supernatants were harvested at regular intervals, passed through a 0.45-μm filter (Whatman), and monitored for virus production by measuring RT activity ((18), details in *SI Text*).

Transmission Electron Microscopy (TEM). Virions were centrifuged through 20% (wt/vol) sucrose, resuspended in 2.5% glutaraldehyde in 0.1 M Sorenson's buffer, and processed for TEM as described (19). Samples were analyzed on a JEOL JEM-1200 EXII electron microscope and photographed using an ORCA-HR digital camera (Hamamatsu). Diameters of 100 virions and cores were measured in Adobe Photoshop.

Anti-XMRV Antisera and Western Blot Analysis. For generation of XMRV whole virus antiserum (anti-XMRV), supernatant from cultured, infected cells was passed through a 0.22-μm filter (Pallcorp); centrifuged (18, 20); lysed with detergent and inoculated into rabbits (details in *SI Text*). The rabbits were bled before inoculation for preimmune control sera. Western blot analysis of concentrated virions was performed as previously described for MoMLV (18–20). XMRV proteins were visualized with primary rabbit anti-XMRV, anti-MoMLV CA (NCI 795-804), anti-MoMLV MA (765-155), anti-MoMLV NC (805008, 1:7,500), and anti-XMRV-SU (1:500) antisera (MoMLV antisera and XMRV anti-XMRV-SU antisera were gifts of J. Rodriguez and S. P. Goff, Columbia University, New York). Data from at least 2 independent Western blots were used to determine XMRV protein sizes by comparison against molecular weight markers. MoMLV (NC_001501) was used for sequence comparisons.

Acquisition of Human Prostate Samples: Cancer and Control Tissues. Radical prostatectomy specimens (n = 233) acquired at the Columbia University Medical Center (CUMC) between August 2006 and December 2007 were used to estimate the prevalence of XMRV in human prostate cancer. Prostate tissues removed by TURP for benign prostatic hyperplasia between January 2007 and April 2008 were used as controls (n = 101). Details of tissue acquisition by banks, specimen selection, and processing are described in *SI Text*. Protected health information was removed and samples were de-identified by the tissue bank. Information about age at time of surgery, ethnicity, tumor stage, and tumor grade was retained (Table S1). Experiments were performed in accordance with the Institutional Review Board of CUMC (IRB-AAAC0089).

DNA Extraction from Human Prostate Tissues. DNA was extracted from 10 sections (10-μm thick) of FFPE tissue, quantified (Nanodrop 1000, Thermo Scientific), and stored at −80 °C (details in *SI Text*).

Quantitative PCR Amplification of Proviral DNA. BLAST analysis of overlapping 250-bp segments of the XMRV genome (VP35, GenBank ID DQ241301.1) identified a region of the integrase gene of XMRV that is 100% conserved between VP35, VP42, and VP62 but shares only 80–85% sequence identity with the most similar murine retroviruses. A forward primer, a hydrolysis probe, and 2 reverse primers were selected from this region using PrimerExpress (Applied Biosystems) (details in Table S2 and *SI Text*).

Immunohistochemistry. FFPE cultured XMRV-infected cells and prostate tissues were sectioned at 5-μm thickness and used for IHC. Details of sectioning, antigen retrieval, antibody treatment, counterstaining, protocol optimization, and controls are in *SI Text*.

RNase L Genotyping. The TaqMan SNP genotyping assay (assay ID: C___935391_1_), with the TaqMan SNP Genotyping Mix (both from Applied Biosystems), were used for RNase L G1385A (R462Q) genotyping (NCBI SNP reference: rs486907). Nine nanograms of prostatic DNA was used in a reaction volume of 20 μL. A TaqMan 7500Fast instrument was used for amplification, detection, and allelic discrimination. *RNASEL* genes from 2 individuals of each genotype were sequenced to confirm allelic discrimination results. DNA from 1 individual of each genotype was used as control in each subsequent experiment.

ACKNOWLEDGMENTS. We thank Drs. J. L. DeRisi and D. Ganem (UCSF) for clones AM-2–9 and AO-H4 and Drs. R. H. Silverman and C. Magi-Galluzzi (Cleveland Clinic) for prostate tissues from patients VP62 and VP45, and Drs. S. P. Goff and J. Rodriguez of Columbia University Medical Center (CUMC) for the XMRV-SU antisera. We thank Drs. H. Hibshoosh and B. Tycko (CUMC) for advice human tissue samples, the staff of the Histology and Immunohistochemistry Laboratories (Pathology Department) and the Tissue Bank (Herbert Irving Comprehensive Cancer Center, both at CUMC), especially S. Alexander, L. Yang, T. Wu, J. Cusmai, and K. Sun. We thank P. M. Pringle for queries of clinical databases, J. Smith for equipment maintenance (both at CUMC), and Drs. M. M. Mansukhani (CUMC) and V. Planelles (University of Utah) for generously sharing space and equipment. We thank Drs. S. P. Goff, V. Planelles, and D. R. Hillyard (University of Utah) for reading of the manuscript. This work was supported by grant PC060433 from the Department of Defense (to I.R.S.).

1. Jemal A, et al. (2008) Cancer statistics, 2008. *CA Cancer J Clin* 58(2):71–96.
2. Hayat MJ, Howlader N, Reichman ME, Edwards BK (2007) Cancer statistics, trends, and multiple primary cancer analyses from the Surveillance, Epidemiology, and End Results (SEER) Program. *Oncologist* 12(1):20–37.
3. Parkin DM, Bray FI, Devesa SS (2001) Cancer burden in the year 2000. The global picture. *Eur J Cancer* 37(Suppl 8):54–566.
4. De Marzo AM, et al. (2007) Inflammation in prostate carcinogenesis. *Nat Rev Cancer* 7(4):256–269.
5. Hayes RB, et al. (2000) Sexual behaviour, STDs and risks for prostate cancer. *Br J Cancer* 82(3):718–725.
6. Urisman A, et al. (2006) Identification of a novel Gammaretrovirus in prostate tumors of patients homozygous for R462Q RNASEL variant. *PLoS Pathog* 2(3):e25.
7. Yeager M, Wilson-Kubalek EM, Weiner SG, Brown PO, Rein A (1998) Supramolecular organization of immature and mature murine leukemia virus revealed by electron cryo-microscopy: Implications for retroviral assembly mechanisms. *Proc Natl Acad Sci USA* 95(13):7299–7304.
8. Casey G, et al. (2002) RNASEL Arg462Gln variant is implicated in up to 13% of prostate cancer cases. *Nat Genet* 32(4):581–583.
9. Fischer N, et al. (2008) Prevalence of human gammaretrovirus XMRV in sporadic prostate cancer. *J Clin Virol* 43(3):277–283.
10. Matsuoka M, Jeang KT (2007) Human T-cell leukaemia virus type 1 (HTLV-1) infectivity and cellular transformation. *Nat Rev Cancer* 7(4):270–280.
11. Grassmann R, Aboud M, Jeang KT (2005) Molecular mechanisms of cellular transformation by HTLV-1 Tax. *Oncogene* 24(39):5976–5985.
12. Cousens C, et al. (2007) In vivo tumorigenesis by Jaagsiekte sheep retrovirus (JSRV) requires Y590 in Env TM, but not full-length orfX open reading frame. *Virology* 367(2):413–421.
13. Dong B, et al. (2007) An infectious retrovirus susceptible to an IFN antiviral pathway from human prostate tumors. *Proc Natl Acad Sci USA* 104(5):1655–1660.
14. Kim S, et al. (2008) Integration site preference of xenotropic murine leukemia virus-related virus, a new human retrovirus associated with prostate cancer. *J Virol* 82(20):9964–9977.
15. Payne GS, et al. (1981) Analysis of avian leukosis virus DNA and RNA in bursal tumours: Viral gene expression is not required for maintenance of the tumor state. *Cell* 23(2):311–322.
16. Andriole GL, et al. (2009) Mortality results from a randomized prostate-cancer screening trial. *N Engl J Med* 360(13):1310–1319.
17. Schroder FH, et al. (2009) Screening and prostate-cancer mortality in a randomized European study. *N Engl J Med* 360(13):1320–1328.
18. Telesnitsky A, Blain S, Goff SP (1995) Assays for retroviral reverse transcriptase. *Methods Enzymol* 262:347–362.
19. Auerbach MR, Brown KR, Singh IR (2007) Mutational analysis of the N-terminal domain of Moloney murine leukemia virus capsid protein. *J Virol* 81(22):12337–12347.
20. Yuan B, Li X, Goff SP (1999) Mutations altering the moloney murine leukemia virus p12 Gag protein affect virion production and early events of the virus life cycle. *EMBO J* 18(17):4700–4710.

the pathophysiology of chytridiomycosis appears to be disruption to the osmoregulatory functioning of the skin and consequent osmotic imbalance that leads to cardiac standstill.

To test whether treating electrolyte abnormalities would reduce the clinical signs of disease, we administered an oral electrolyte supplement to *L. caerulea* in the terminal stages of infection, when they lost the righting reflex and could no longer correct their body positions (*26*). Frogs under treatment recovered a normal posture and became more active; one individual recovered sufficiently to climb out of the water onto the container walls, and two individuals were able to jump to avoid capture. These signs of recovery were not observed in any untreated frogs. In addition, treated frogs lived >20 hours longer than untreated frogs [mean time after treatment ± SEM: treated frogs (N = 9), 32 ± 2.8 hours; control frogs (N = 6), 10.7 ± 2.2 hours; Student's t test, $P < 0.001$]. All treated frogs continued to shed skin and ultimately died from the infection, as expected. It is unlikely that electrolyte treatment could prevent death unless the epidermal damage caused by *Bd* is reversed. Although amphibians can generally tolerate greater electrolyte fluctuations than other terrestrial vertebrates (*18*), we suggest that depletion of electrolytes, especially potassium, is important in the pathophysiology of chytridiomycosis. Amphibian plasma potassium concentrations are maintained at constant levels across seasons (*27*), and even moderate hypokalemia is dangerous in humans (*28*).

Our results support the epidermal dysfunction hypothesis, which suggests that *Bd* disrupts cutaneous osmoregulatory function, leading to electrolyte imbalance and death. The ability of *Bd* to compromise the epidermis explains how a superficial skin fungus can be fatal to many species of amphibians; their existence depends on the physiological interactions of the skin with the external environment (*16*–*19*). Disease outbreaks capable of causing population declines require the alignment of multiple variables, including a life-compromising pathophysiology (*1*). Resolving the pathogenesis of chytridiomycosis is a key step in understanding this unparalleled pandemic.

References and Notes

1. P. Daszak, A. A. Cunningham, A. D. Hyatt, *Divers. Distrib.* **9**, 141 (2003).
2. F. de Castro, B. Bolker, *Ecol. Lett.* **8**, 117 (2005).
3. L. Berger *et al.*, *Proc. Natl. Acad. Sci. U.S.A.* **95**, 9031 (1998).
4. D. B. Wake, V. T. Vredenburg, *Proc. Natl. Acad. Sci. U.S.A.* **105**, 11466 (2008).
5. H. McCallum, *Conserv. Biol.* **19**, 1421 (2005).
6. K. R. Lips *et al.*, *Proc. Natl. Acad. Sci. U.S.A.* **103**, 3165 (2006).
7. L. F. Skerratt *et al.*, *EcoHealth* **4**, 125 (2007).
8. L. M. Schloegel *et al.*, *EcoHealth* **3**, 35 (2006).
9. D. C. Woodhams, R. A. Alford, *Conserv. Biol.* **19**, 1449 (2005).
10. K. M. Mitchell, T. S. Churcher, T. W. J. Garner, M. C. Fisher, *Proc. R. Soc. London Ser. B* **275**, 329 (2008).
11. M. Schaechter, B. I. Eisensteing, G. Medoff, in *Mechanisms of Microbial Disease* (Williams & Wilkins, Baltimore, 1998), pp. 419–439.
12. J. E. Longcore, A. P. Pessier, D. K. Nichols, *Mycologia* **91**, 219 (1999).
13. L. Berger *et al.*, *Dis. Aquat. Organ.* **68**, 65 (2005).
14. D. C. Woodhams *et al.*, *Anim. Conserv.* **10**, 409 (2007).
15. E. B. Rosenblum, J. E. Stajich, N. Maddox, M. B. Eisen, *Proc. Natl. Acad. Sci. U.S.A.* **105**, 17034 (2008).
16. H. Heatwole, in *Amphibian Biology, Vol. 1. The Integument*, H. Heatwole, G. T. Barthalmus, Eds. (Surrey Beatty, Chipping Norton, New South Wales, 1994), pp. 98–168.
17. R. G. Boutilier, D. F. Stiffler, D. P. Toews, in *Environmental Physiology of the Amphibians*, M. E. Feder, W. W. Burggren, Eds. (Univ. of Chicago Press, Chicago, 1992), pp. 81–124.
18. I. J. Deyrup, in *Physiology of the Amphibia*, J. A. Moore, Ed. (Academic Press, New York, 1964), vol. 1, pp. 251–315.
19. K. M. Wright, B. R. Whitaker, in *Amphibian Medicine and Captive Husbandry*, K. M. Wright, B. R. Whitaker, Eds. (Krieger, Malabar, FL 2001), pp. 318–319.
20. J. Voyles *et al.*, *Dis. Aquat. Organ.* **77**, 113 (2007).
21. L. Berger, G. Marantelli, L. F. Skerratt, R. Speare, *Dis. Aquat. Organ.* **68**, 47 (2005).
22. D. J. Benos, L. J. Mandel, R. S. Balaban, *J. Gen. Physiol.* **73**, 307 (1979).
23. R. H. Alvarado, T. H. Dietz, T. L. Mullen, *Am. J. Physiol.* **229**, 869 (1975).
24. G. A. Castillo, G. G. Orce, *Comp. Biochem. Physiol. A* **118**, 1145 (1997).
25. N. A. Paradis, H. R. Halperin, R. M. Nowak, in *Cardiac Arrest: The Science and Practice of Resuscitation Medicine* (Williams & Wilkins, Baltimore, 1996), pp. 621–623.
26. See supporting material on *Science* Online.
27. D. R. Robertson, *Comp. Biochem. Physiol. A* **60**, 387 (1978).
28. F. J. Gennari, *N. Engl. J. Med.* **339**, 451 (1998).
29. We thank A. Hyatt and V. Olsen for assistance with PCR and S. Bell, J. Browne, S. Cashins, S. Garland, M. Holdsworth, C. Manicom, L. Owens, R. Puschendorf, K. Rose, E. Rosenblum, D. Rudd, A. Storfer, J. VanDerwal, B. Voyles, and J. Warner for project assistance and editing. Supported by Australian Research Council Discovery Project grant DP0452826, Australian Government Department of Environment and Heritage grant RFT 43/2004, and the Wildlife Preservation Society of Australia. Animals were collected with permission from Queensland Parks and Wildlife Service (scientific permits WISP03866106 and WISP04143907; movement permit WTWM04381507) and New South Wales Parks and Wildlife Service (import license !E0705693).

Supporting Online Material

www.sciencemag.org/cgi/content/full/326/5952/582/DC1
Materials and Methods
SOM Text
Figs. S1 and S2
Tables S1 and S2
References

26 May 2009; accepted 26 August 2009
10.1126/science.1176765

Detection of an Infectious Retrovirus, XMRV, in Blood Cells of Patients with Chronic Fatigue Syndrome

Vincent C. Lombardi,[1]* Francis W. Ruscetti,[2]* Jaydip Das Gupta,[3] Max A. Pfost,[1] Kathryn S. Hagen,[1] Daniel L. Peterson,[1] Sandra K. Ruscetti,[4] Rachel K. Bagni,[5] Cari Petrow-Sadowski,[6] Bert Gold,[2] Michael Dean,[2] Robert H. Silverman,[3] Judy A. Mikovits[1]†

Chronic fatigue syndrome (CFS) is a debilitating disease of unknown etiology that is estimated to affect 17 million people worldwide. Studying peripheral blood mononuclear cells (PBMCs) from CFS patients, we identified DNA from a human gammaretrovirus, xenotropic murine leukemia virus–related virus (XMRV), in 68 of 101 patients (67%) as compared to 8 of 218 (3.7%) healthy controls. Cell culture experiments revealed that patient-derived XMRV is infectious and that both cell-associated and cell-free transmission of the virus are possible. Secondary viral infections were established in uninfected primary lymphocytes and indicator cell lines after their exposure to activated PBMCs, B cells, T cells, or plasma derived from CFS patients. These findings raise the possibility that XMRV may be a contributing factor in the pathogenesis of CFS.

Chronic fatigue syndrome (CFS) is a disorder of unknown etiology that affects multiple organ systems in the body. Patients with CFS display abnormalities in immune system function, often including chronic activation of the innate immune system and a deficiency in natural killer cell activity (*1*, *2*). A number of viruses, including ubiquitous herpesviruses and enteroviruses, have been implicated as possible environmental triggers of CFS (*1*). Patients with CFS often have active β herpesvirus infections, suggesting an underlying immune deficiency.

The recent discovery of a gammaretrovirus, xenotropic murine leukemia virus–related virus (XMRV), in the tumor tissue of a subset of prostate cancer patients prompted us to test whether XMRV might be associated with CFS. Both of these disorders, XMRV-positive prostate cancer and CFS, have been linked to alterations in the antiviral enzyme RNase L (*3*–*5*). Using the Whittemore Peterson Institute's (WPI's) national

[1]Whittemore Peterson Institute, Reno, NV 89557, USA. [2]Laboratory of Experimental Immunology, National Cancer Institute–Frederick, Frederick, MD 21701, USA. [3]Department of Cancer Biology, The Lerner Research Institute, The Cleveland Clinic Foundation, Cleveland, OH 44195, USA. [4]Laboratory of Cancer Prevention, National Cancer Institute–Frederick, Frederick, MD 21701, USA. [5]Advanced Technology Program, National Cancer Institute–Frederick, Frederick, MD 21701, USA. [6]Basic Research Program, Scientific Applications International Corporation, National Cancer Institute–Frederick, Frederick, MD 21701, USA.

*These authors contributed equally to this work.
†To whom correspondence should be addressed. E-mail: judym@wpinstitute.org